

Single light scattering: Bubbles versus droplets

Alexander A. Kokhanovsky^{a)}

*Institute of Environmental Physics, Bremen University, P.O. Box 330440, Bremen, Germany
and Institute of Physics, Minsk 220072, Belarus*

(Received 6 March 2003; accepted 27 August 2003)

The intensity and polarization characteristics of scattered light beams are studied for bubbles in water and compared to the case of water droplets in air. The size distributions of the scatters in both systems are assumed to be the same. It is shown that spherical polydispersions of water droplets give generally larger depolarization effects than bubbles, leading to larger entropy production by droplets than bubbles. © 2004 American Association of Physics Teachers.

[DOI: 10.1119/1.1621030]

I. INTRODUCTION

The interaction of light with macroscopic liquid or solid particles can be studied in the framework of Mie theory.¹ Usually one is interested in the scattered light intensity and polarization characteristics as functions of the scattering angle, particle sizes or shapes, and their refractive indices.^{2–4} The goal of this paper is to identify differences in light scattering that are due to different types of mixtures of the same substances.

In particular, we consider the case of air bubbles in water and water droplets in air. Our results are of interest for studies of light propagation through a cloudy atmosphere and the ocean. In particular, bubble clouds play an essential role in radiative transport close to the ocean surface, especially if a strong wind is present. Above the ocean surface there is a cloud of droplets and below it bubble clouds develop.

Droplets in clouds and bubbles in water are usually much larger than the wavelength of visible light. They also are polydisperse. Our calculations are for spherical polydispersions with the following particle size distribution, which is frequently used for studies of light propagation in clouds:³

$$f(a) = A a^6 \exp(-0.6a), \quad (1)$$

where $A = 3^5 / (2^4 \times 5^8)$, which insures that

$$\int_0^\infty f(a) da = 1. \quad (2)$$

Asymmetric distributions such as those given by Eq. (1) are typical for water droplets in terrestrial clouds.^{3,4} Note that the mode radius a_0 in Eq. (1) is equal to 10 μm. The mode radius is defined in such a way that the function in Eq. (1) has a maximum at this radius. Note that a_0 is much larger than the wavelength of the incident light λ used in the calculations ($\lambda = 0.55 \mu\text{m}$).

II. THEORY

The problem of electromagnetic wave interaction with a single macroscopic spherical particle (for example, a cloud droplet) was solved roughly a century ago (see, for example, Ref. 1). The solution in the far field can be written in terms of the Stokes vector parameter of the scattered radiation \vec{S} (S_1, S_2, S_3, S_4),^{2–4}

$$\vec{S} = \frac{\Phi(\theta)}{k^2 r^2} \vec{S}_0, \quad (3)$$

where θ is the scattering angle, $k = 2\pi/\lambda$, λ is the wavelength, r is the distance to the observation point, and \vec{S}_0 is the Stokes vector parameter of the incident light. Note that the components of the Stokes vector parameter are defined as bilinear combinations of the correspondent electric field vector $\vec{E} = E_1 \vec{i} + E_2 \vec{j}$.^{2–4} The vector $\vec{k} = \vec{j} \times \vec{i}$ gives the direction of the electromagnetic wave propagation. Namely, we have^{2–4} $S_1 = E_1 E_2^* + E_2 E_1^*$, $S_2 = E_1 E_1^* - E_2 E_2^*$, $S_3 = E_1 E_2^* + E_1^* E_2$, $S_4 = i(E_1 E_2^* - E_1^* E_2)$, where we neglected a common multiplier. In electromagnetic scattering problems, it is usually assumed that the vector \vec{i} is in the plane of scattering, and the vector \vec{j} is in the plane perpendicular to the plane of scattering.

The nonzero elements of the 4×4 scattering matrix $\hat{\Phi}$ for spheres can be calculated using the following equations:^{2–4}

$$\Phi_{11} = \Phi_{22} = \frac{1}{2} [|A_{11}|^2 + |A_{22}|^2], \quad (4)$$

$$\Phi_{12} = \Phi_{21} = \frac{1}{2} [|A_{11}|^2 - |A_{22}|^2], \quad (4)$$

$$\Phi_{33} = \Phi_{44} = \text{Re}[A_{11} A_{22}^*], \quad (5)$$

$$\Phi_{34} = -\Phi_{43} = \text{Im}[A_{11} A_{22}^*], \quad (5)$$

where A_{11} and A_{22} are elements of the amplitude scattering matrix

$$\hat{A} = \begin{pmatrix} A_{11} & 0 \\ 0 & A_{22} \end{pmatrix} \quad (6)$$

and^{2–4}

$$A_{11} = \sum_{j=1}^{\infty} \frac{2j+1}{j(j+1)} [a_j \tau_j + b_j \pi_j], \quad (7)$$

$$A_{22} = \sum_{j=1}^{\infty} \frac{2j+1}{j(j+1)} [a_j \pi_j + b_j \tau_j]. \quad (7)$$

Here π_j is the derivative of the Legendre polynomial $P_j(\cos \theta)$ and τ_j is the derivative of the associated Legendre polynomial $P_j^1(\cos \theta)$ with respect to $\cos \theta$. The amplitude coefficients a_j and b_j are given by complex combinations of the spherical Bessel functions, which depend on the complex refractive index of particles and the ratio a/λ .² Both Legendre polynomials and spherical Bessel functions can be

Table I. The physical meaning of the normalized scattering matrix elements [see Eq. (8)].

| Stokes vector of the incident light | Stokes vector of the scattered light for spherical polydispersion | Degree of polarization |
|---|---|---------------------------------------|
| Unpolarized light | Partially linearly polarized light | Linear polarization |
| $\begin{pmatrix} 1 \\ 0 \\ 0 \\ 0 \end{pmatrix}$ | $\begin{pmatrix} \Phi_{11} \\ \Phi_{12} \\ 0 \\ 0 \end{pmatrix}$ | $p_l = -\frac{\Phi_{12}}{\Phi_{11}}$ |
| Right circularly polarized light | Partially circularly polarized light | Circular polarization |
| $\begin{pmatrix} 1 \\ 0 \\ 0 \\ 1 \end{pmatrix}$ | $\begin{pmatrix} \Phi_{11} \\ 0 \\ 0 \\ \Phi_{44} \end{pmatrix}$ | $p_c = \frac{\Phi_{44}}{\Phi_{11}}$ |
| Linearly polarized light with the azimuth -45° | Partially elliptically polarized light | Circular polarization |
| $\begin{pmatrix} 1 \\ 0 \\ -1 \\ 0 \end{pmatrix}$ | $\begin{pmatrix} \Phi_{11} \\ \Phi_{11} \\ -\Phi_{33} \\ \Phi_{34} \end{pmatrix}$ | $p_c^* = \frac{\Phi_{34}}{\Phi_{11}}$ |

found using standard recurrence formulas. The corresponding equations can be found in Refs. 2–4.

It should be stressed that the elements of the matrix $\hat{\Phi}$ are easily measured using different illumination conditions as summarized in Table I. It follows from Table I that the elements of the normalized scattering matrix $\hat{p} = \hat{\Phi}/\Phi_{11}$ have a clear physical meaning. Namely, it follows that

$$\hat{p} = \begin{pmatrix} 1 & -p_l & 0 & 0 \\ -p_l & 1 & 0 & 0 \\ 0 & 0 & p_c & p_c^* \\ 0 & 0 & -p_c^* & p_c \end{pmatrix}, \quad (8)$$

where p_l is the degree of linear polarization of scattered light assuming the illumination of a particle by unpolarized light and p_c and p_c^* are the degrees of circular polarization of scattered light assuming circularly or linearly (with the azimuth equal to -45°) polarized incident light, respectively.⁴ The matrix (8) plays an important role in radiative transfer problems.^{3,4} We will consider the elements of this matrix in the following.

Another important characteristic is the total scattered intensity for the illumination of a particle by unpolarized light. Its angular distribution is given by Φ_{11} [see Eq. (3) and Table I]. We will consider, however, not Φ_{11} , but the phase function

$$p(\theta) = \frac{4\pi\Phi_{11}(\theta)}{C_{\text{sca}}k^2}, \quad (9)$$

where

$$C_{\text{sca}} = \frac{2\pi}{k^2} \int_0^\pi \Phi_{11}(\theta) \sin \theta d\theta \quad (10)$$

is the scattering cross section.^{2–4} The integral (10) can be calculated analytically. The result is²

$$C_{\text{sca}} = \frac{2\pi}{k^2} \sum_{j=1}^{\infty} (2j+1)(|a_j|^2 + |b_j|^2). \quad (11)$$

Note that it follows by definition: $\frac{1}{2} \int_0^\pi p(\theta) \sin \theta d\theta = 1$. Therefore, the phase function gives the conditional probability of light scattering in a fixed direction.⁴

Equations (4)–(7), (9)–(11) are valid for monodisperse scatterers only. The conversion to the polydispersed case is straightforward.³ We need to substitute Φ_{ij} and C_{sca} by the average values $\langle \Phi_{ij} \rangle$ and $\langle C_{\text{sca}} \rangle$. The angular brackets have the following meaning:

$$\langle Y \rangle = \int_0^\infty Y(a) f(a) da. \quad (12)$$

III. RESULTS OF NUMERICAL CALCULATIONS

The results of calculations of the phase function $p(\theta)$, which gives the conditional probability of light scattering in the direction specified by the scattering angle θ , are shown in Fig. 1(a). This result was found using Eqs. (9), (4), (11), and (7). The function $\Phi_{11}(\theta)$ and the value of C_{sca} in Eq. (9) were averaged according to Eq. (12) with the particle size distribution (1).

We see that $p(\theta)$ is quantitatively and qualitatively different for bubbles and droplets. In particular there is no rainbow scattering for bubbles as there is with droplets (see the angle range 120° – 160°). There is an increase in the phase function as $\theta \rightarrow \pi$ for droplets, but this increase is not as pronounced for bubbles. The probability of photon scattering by bubbles in the region from 120° to 180° is considerably smaller for bubbles than droplets. Thus, the backscattered signal from bubbles is comparatively weak. On the other hand, bubbles are stronger scatterers at the lateral angles (from 40° to 110°). Due to the same size of the droplets and bubbles in

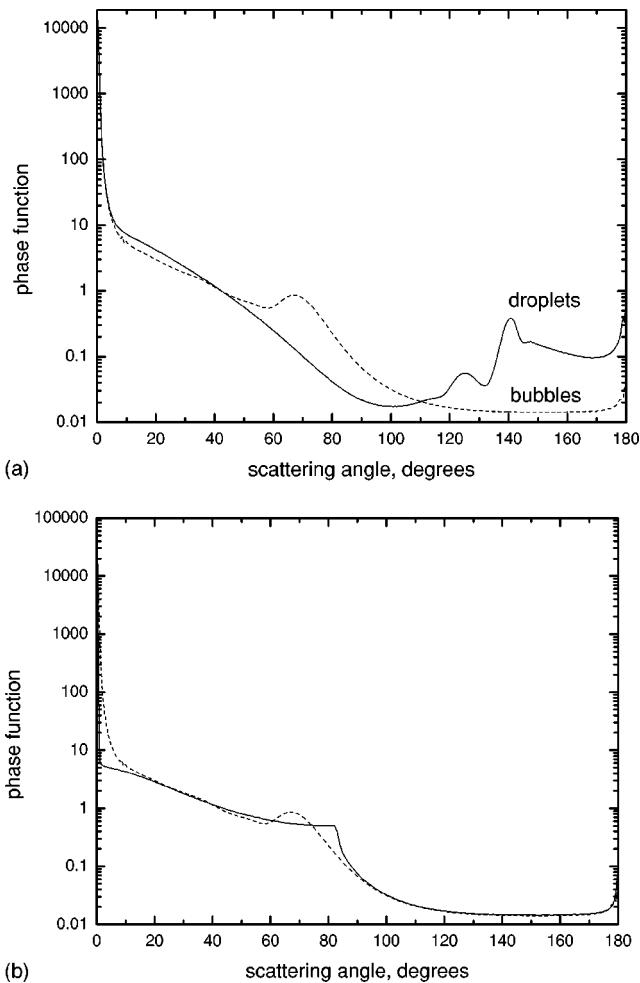


Fig. 1. (a) The phase function of water droplets in air (solid line) and air bubbles in water (dashed line). The particle size distribution is given by Eq. (1). The wavelength is equal to $0.55 \mu\text{m}$. (b) The phase function of air bubbles in water, calculated using the geometric optics approach for a single bubble (Ref. 2), with a radius 1 mm (solid line). The results given by the dashed lines in (a) and (b) coincide.

our model, their phase functions coincide when $\theta < \theta_d$, where $\theta_d = 5^\circ$ in the case studied. The range $[0, \theta_d]$ specifies the diffraction zone.

There is an interesting feature in the behavior of the phase function of bubbles when the scattering angle is close to 70° . This feature is related to the fact that rays incident on spherical particles (with refractive indices $n < 1$) at angles larger than the critical angle $\varphi = \arcsin(n)$ do not penetrate inside the particles.⁵ The critical scattering angle θ_c is related to the critical angle φ by² $\theta_c = \pi - 2\varphi$. This gives for the critical scattering angle $\theta_c = 82.82^\circ$ for $n = 0.75$. Light scattering at $\theta_d < \theta < \theta_c$ is mostly due to the total internal light reflection from the surfaces of the bubbles. Detailed studies of wave effects at angles close to θ_c [see Fig. 1(a)] were performed by Fiedler-Ferrari *et al.*⁵

We compare our calculated results using geometric optics² (valid for $a/\lambda \rightarrow \infty$) for the phase function of bubbles to those using wave optics in Fig. 1(b). This comparison suggests that the case studied ($a_0 = 10 \mu\text{m}$) is very close to the asymptotic geometric optics scattering regime in the backward hemisphere. However, there are differences in the region near θ_c , where total internal reflection takes place.⁵ The

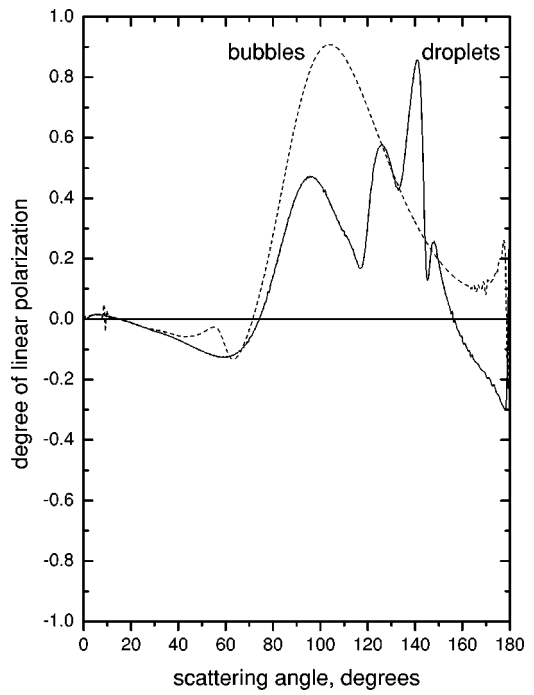


Fig. 2. The angular dependence of the degree of linear polarization p_l of scattered light for the same conditions as in Fig. 1(a).

differences as $\theta \rightarrow 0$ in Fig. 1(b) are due to different values of a_0 of particles assumed for the geometric optics case ($a_0 = 1000 \mu\text{m}$) and Mie theory ($a_0 = 10 \mu\text{m}$) calculations.

The position of the step around 80° [see Fig. 1(b)] depends on the particle size and the wavelength. Therefore, white light scattered around this angle will be colored.

The degree of linear polarization p_l of scattered light for initially unpolarized incident light beam is given in Fig. 2. It was calculated using the corresponding equation in Table I. The elements Φ_{11} and Φ_{12} [see Eq. (4)] were averaged according to Eq. (12) with the particle size distribution (1).

We see that p_l is rather small both for bubbles and droplets in the forward scattering region (below 90°). It increases for larger angles and is larger for bubbles everywhere in the backward hemisphere except in regions where rainbow (around 140°) and glory scattering (around 180°) occurs for water droplets. Interestingly, the value of p_l for bubbles is positive in the backward hemisphere (except at a narrow angle range near 180°). It is negative, however, for droplets at scattering angles larger than 155° . It becomes positive for droplets again around the backward ($\theta = \pi$) scattering directions. We see that both bubbles and droplets show the change of the sign of p_l at the glory scattering region. Generally, the angular dependence of $p_l(\theta)$ is much smoother for bubbles than for droplets.

We present the degree of circular polarization $p_c(\theta)$ of singly scattered light in Figs. 3(a) and 3(b). It has been calculated using the corresponding equation in Table I. The elements Φ_{11} and Φ_{44} [see Eqs. (4) and (5)] were averaged according to Eq. (12) with the particle size distribution (1). The case given in Fig. 3(a) corresponds to incident light that is completely right circularly polarized ($p_c = 1$). We see that both bubbles and droplets do not significantly change the degree of polarization for angles smaller than 20° . They both convert incident right circularly polarized light ($p_c = 1$) into

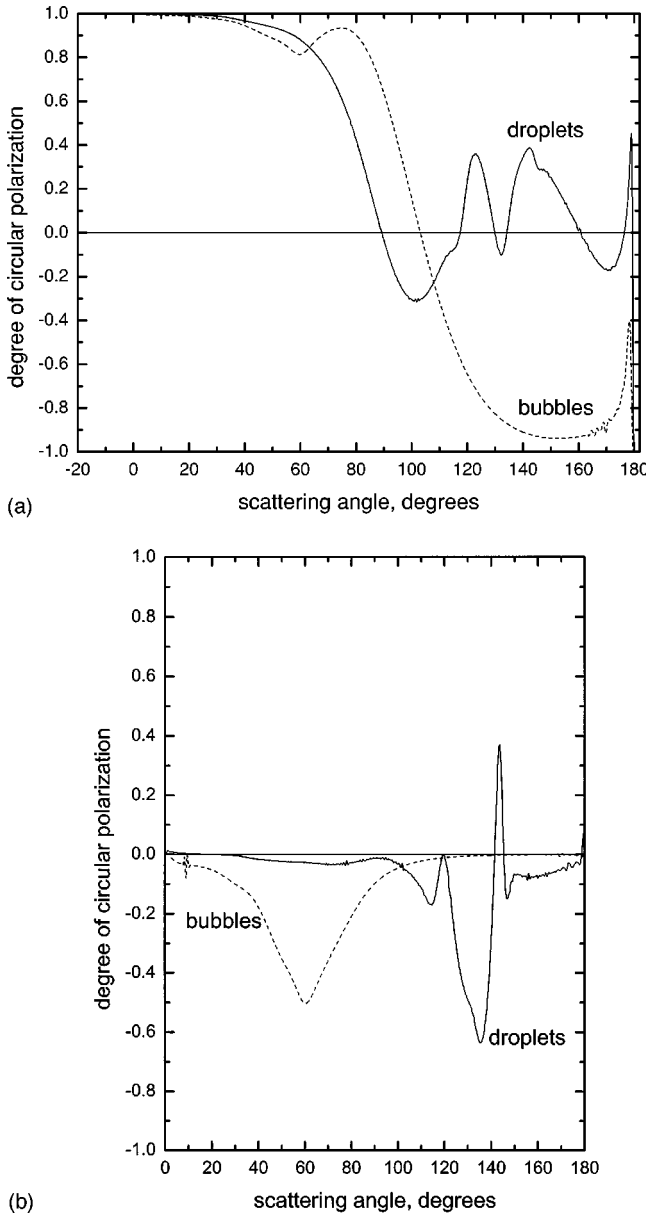


Fig. 3. (a) The same as in Fig. 2, but for the degree of circular polarization p_c . (b) The same as in Fig. 2, but for the degree of circular polarization p_c^* .

left circularly polarized light ($p_c = -1$) at a 180° scattering angle. The curve $p_c(\theta)$ is much smoother for bubbles compared to droplets. It crosses the line $p_c = 0$ only once in contrast to droplets, where the degree of circular polarization of scattered light p_c vanishes at seven scattering angles, therefore, producing partially linearly polarized light ($p_c = 0$).

Bubbles change the sense of rotation of the electric vector at angles larger than 105° ($p_c < 0$). Droplets are characterized by different signs of $p_c(\theta)$ depending on the specific scattering angle interval in the backward hemisphere.

The degree of circular polarization $p_c^*(\theta)$ of scattered light for incident linearly polarized light (the azimuth angle $\psi = 45^\circ$) is given in Fig. 3(b). It was calculated using the corresponding equation in Table I. The elements Φ_{11} and Φ_{34} [see Eqs. (4) and (5)] were averaged as before.

The value of p_c^* is close to zero for bubbles and it is in the range $[-0.65, 0.4]$ for water droplets in the backward hemi-

sphere. On the other hand, the value p_c^* for droplets is close to zero in the forward scattering hemisphere in comparison to larger values of p_c^* for bubbles [see Fig. 3(b)]. Larger values of p_c^* mean that bubbles can easily convert linearly polarized light in the circular polarization mode in the forward scattering region in contrast to droplets. Droplets give large negative values of p_c^* at the rainbow angle.

The values of the asymmetry parameters $g = 0.25 \int_0^\pi p(\theta) \sin 2\theta d\theta$ for both droplets and bubbles are close (~ 0.85). This means that thick layers of both clouds and bubbles of the same optical thickness will have similar values of the diffuse transmittance and reflection coefficients.⁶ Such a behavior is in contrast to the differences in singly scattered light characteristics shown in Figs. 1–3.

IV. THE ENTROPY OF SCATTERED LIGHT

We briefly discuss the difference in entropy of light beams scattered by bubbles and droplets. The maximum entropy principle is a central organizing principle of statistical physics. The entropy of a radiation field is considered in Refs. 7 and 8. The concept of entropy allows us to introduce a thermodynamic approach to the problems of polarization optics.^{8,9} In particular, entropy calculations play an important role in the analysis of the irreversible evolution of the multiply scattered light by a random medium.¹⁰

The entropy s of the radiation field is defined as¹¹

$$s = -\text{Tr}(\hat{D} \ln \hat{D}), \quad (13)$$

where Tr means the trace operation and \hat{D} is the density matrix. Equation (13) is a standard definition used in statistical mechanics. Equation (13) can be reduced to⁸

$$s = -\ln(\alpha^\alpha \beta^\beta), \quad (14)$$

where $\alpha = (1 + \Pi)/2$ and $\beta = (1 - \Pi)/2$ are eigenvalues⁸ of the density matrix. The value of Π gives the degree of total polarization, defined as $\sqrt{S_2^2 + S_3^2 + S_4^2}/S_1$.⁸ Note that Eq. (14) also can be written as

$$s = -\ln[0.5(1 + \Pi)^\alpha(1 - \Pi)^\beta]. \quad (15)$$

Consider the illumination of a spherical polydispersion by a linearly polarized light beam with the azimuth angle $\psi = -45^\circ$. Then we have (see Table I):

$$\Pi = \sqrt{p_l^2 + p_c^2 + p_c^{*2}}. \quad (16)$$

Π is exactly equal to unity for monodispersed spheres, which can be easily shown using Eqs. (4), (5), and Table I. Therefore, the difference, $\Delta = \Pi - 1$, shows the influence of polydispersity on the value of the degree of total polarization Π . Note that we have for monodispersed spheres [see Eq. (15)] $s = 0$, which means that single scattering by monodispersed spheres does not produce entropy of scattering beams. The entropy is due to the polydispersity of the medium or multiple scattering effects.

We have for a completely polarized light beam ($\Pi = 1$), $s = 0$, independent of the specific type of polarization (linear, elliptic or circular). For unpolarized beams ($\Pi = 0$), the entropy is a maximum and, therefore, $s = \ln 2$.

The function $\Pi(\theta)$ is shown in Fig. 4. The value of Π remains larger than 0.9 for bubbles for almost all scattering

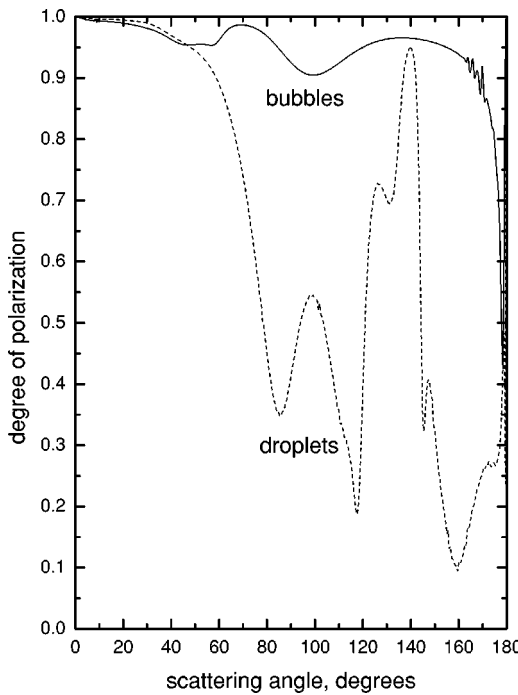


Fig. 4. The same as in Fig. 2, but for the degree of polarization Π .

angles (except the glory scattering region, where it drops to 0.4). It is smaller for droplets with three distinctive minima at approximately 85° , 118° , and 160° . For the last minimum, the value of Π drops below 0.1. Therefore, at this angle, around 90% of the incident completely polarized light is transformed to completely unpolarized light. Note that $\Pi = 1$ in the exact forward and backward scattering directions because $A_{11} = A_{22}$ at $\theta = 0$ and $A_{11} = -A_{22}$ at $\theta = \pi$ [see Eqs. (4)–(7), (9), and Table I].

The angular dependence of the entropy of scattered light is presented in Fig. 5, which was derived from data given in Fig. 4 using Eq. (15). We note that Fig. 4 corresponds to a completely polarized incident light beam ($s=0$). The entropy of scattered beam is not equal to zero, however. The entropy production $\Delta s = s_2 - s_1$, where s_1 gives the entropy of incident beam and s_2 is the entropy of scattered beam, generally increases with the scattering angle. It drops at the rainbow (for droplets) and glory regions due to the high polarizing ability of particles in these regions. The entropy production is equal to zero at exact forward and backward scattering regions. Spherical particles do not depolarize incident completely polarized light in these directions.

V. CONCLUSION

In this paper, the author has contrasted the intensity and polarization characteristics of scattered light beams for ensembles of droplets in air and air bubbles in water. The scattering by such systems differs considerably even if the scatterers have exactly the same size. Thus, results obtained for droplets cannot be generalized to bubbly media and vice versa. The calculations were performed for a single particle size distribution $f(a)$. However, our results are valid [at least, qualitatively, see Fig. 1(b)] for all nonabsorbing particles with $a \gg \lambda$. They can be used as input for the solution of the vector radiative transfer equation⁴ for cloudy and bubbly media.

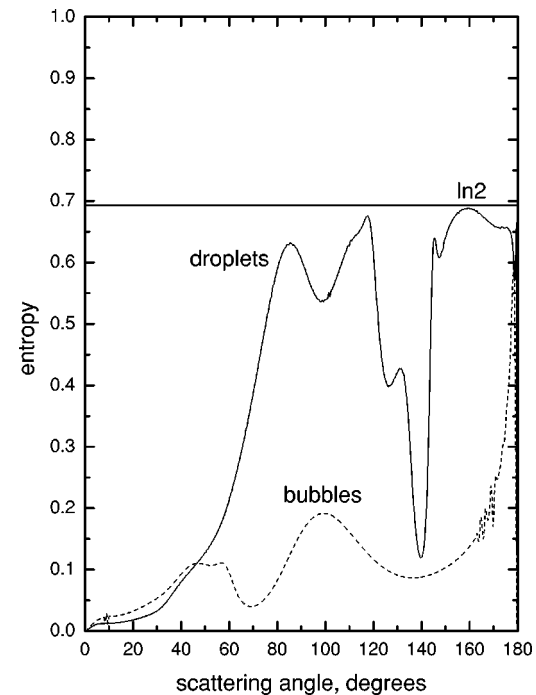


Fig. 5. The same as in Fig. 2 but for the scattered light beam entropy s .

The angular dependence of the entropy of scattered light beam for bubbles and water droplets has been studied. Droplets are far more effective producers of entropy in comparison to bubbles. The use of the notion of entropy and especially the principle of its maximum can lead to further advances in the field of polarization optics. In particular, it may be the goal of optical design to construct a measurement system with $\Delta s = 0$.⁸

The author emphasizes that the Mie theory is not normally discussed in the graduate or undergraduate curriculum. However, because light scattering by a sphere has such a long list of applications,² physicists should be aware of the subject. In particular, light scattering by aerosols and clouds is one of the central issues of modern satellite remote sensing of the terrestrial troposphere,⁴ and is important, for example, for global warming issues. The extension of the research given here (especially as far as the entropy of the scattered light is concerned) would make an excellent student project and help students learn about the field of light scattering by small macroscopic particles.

ACKNOWLEDGMENTS

This work was supported by the Institute of Environmental Physics (Bremen University). The author thanks A. Macke for the use of his Monte Carlo code, which was used to generate the solid line in Fig. 1(b).

^aElectronic mail: alexk@iup.physik.uni-bremen.de

¹G. Mie, "Beitrage zur Optik truber Medien speziell kolloidaler Metallösungen," Ann. Phys. (Leipzig) **25**, 377–445 (1908).

²H. C. Van de Hulst, *Light Scattering by Small Particles* (Dover, New York, 1981).

³D. Deirmendjian, *Electromagnetic Light Scattering on Spherical Polydispersions* (Elsevier, Amsterdam, 1969).

⁴A. Kokhanovsky, *Optics of Light Scattering Media* (Springer-Praxis, Chichester, 2001).

⁵N. Fiedler-Ferrari, H. M. Nussenzveig, and W. J. Wiscombe, "Theory of

near-critical-angle scattered from a curved interface," Phys. Rev. A **43**, 1005–1038 (1991).

⁶A. Kokhanovsky, "Optics of turbid slabs," Eur. J. Phys. **23**, 27–33 (2002).

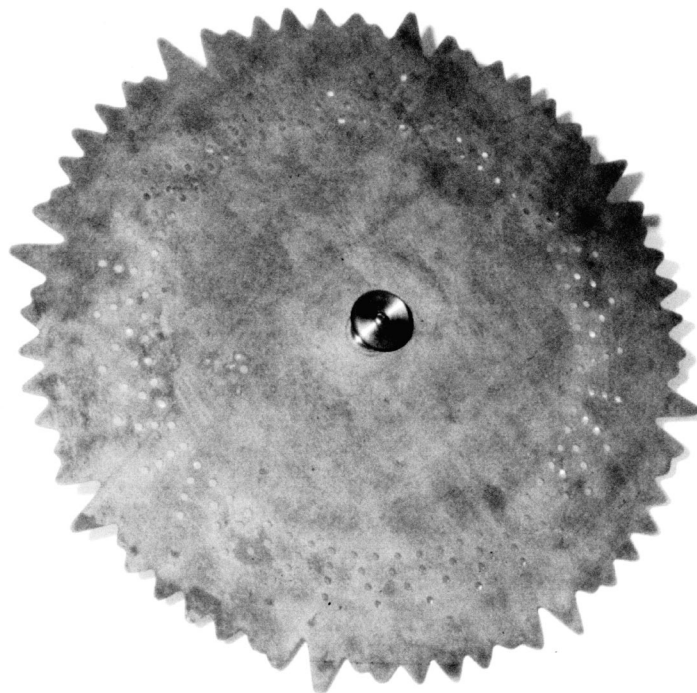
⁷M. Planck, *Vorlesungen über die Theorie der Warmestrahlung* (Barth, Leipzig, 1923).

⁸C. Brosseau, *Fundamentals of Polarized Light: A Statistical Approach* (Wiley, New York, 1998).

⁹A. Kokhanovsky, *Polarization Optics of Random Media* (Springer-Praxis, Berlin, 2003).

¹⁰C. Brosseau and D. Bicout, "Entropy production in multiple scattering of light by a spatially random medium," Phys. Rev. E **50**, 4997–5005 (1994).

¹¹J. von Neumann, *Mathematical Foundations of Quantum Mechanics* (Princeton University Press, Princeton, NJ, 1955).



Siren Disk. This disk was used for Fourier synthesis. "This edge of the disk before you answers to a curve corresponding to a tone compounded of a prime and four perturbed harmonic partials. The fundamental consists of 24 waves. The first upper partial consists of 49 waves ($2 \times 24 + 1$); the second of 75 ($3 \times 24 + 3$); the third of 101 ($4 \times 24 + 5$); and the fourth of 127 waves ($5 \times 24 + 7$)... When air is blown through a narrow slit against the teeth of this disk, a very disagreeable and slightly intermittent sound is the result." From J. A. Zahm, *Sound and Music*, second edition (Chicago, A. C. McClurg & Co.), p. 381. The disk was made by Rudolph Koenig of Paris, and is in the apparatus collection at the University of Vermont. (Photograph and notes by Thomas B. Greenslade, Jr., Kenyon College)